Observation of multiple sub-cavities adjacent to single separatrix

Rongsheng Wang,[1] Aimin Du,[1] Rumi Nakamura,[2] Quanming Lu,[3] Yuri V. Khotyaintsev,[4] Martin Volwerk,[2] Tielong Zhang,[2] E. A. Kronberg,[5] P. W. Daly,[5] and Andrew N. Fazakerley[6]

[1] We investigate a direct south-north crossing of a reconnection ion diffusion region in the magnetotail. During this crossing, multiple electron density dips with a further density decrease within the cavity, called sub-cavities, adjacent to the northern separatrix are observed. The correlation between electron density sub-cavities and strong electric field fluctuations is obvious. Within one of the sub-cavities, a series of very strong oscillating perpendicular electric field and patchy parallel electric field are observed. The parallel electric field is nearly unipolar and directs away from X line. In the same region, inflow electrons with energy up to 100 keV are injected into the X line. Based on the observations, we conclude that the high-energy inflowing electrons are accelerated by the patchy parallel electric field. Namely, electrons have been effectively accelerated while they are flowing into the X line along the separatrix. The observations indicate that the electron acceleration region is widely larger than the predicted electron diffusion region in the classical Hall magnetic reconnection model. **Citation:** Wang, R., A. Du, R. Nakamura, Q. Lu, Y. V. Khotyaintsev, M. Volwerk, T. Zhang, E. A. Kronberg, P. W. Daly, and A. N. Fazakerley (2013), Observation of multiple sub-cavities adjacent to single separatrix, *Geophys. Res. Lett.*, *40*, doi:10.1002/grl.50537.

1. Introduction

[2] Magnetic reconnection is a fundamental plasma process in space and laboratory plasmas, by which stored magnetic energy is converted into plasma energy, and mass and momentum are transferred across boundaries. In the Earth magnetosphere, it frequently happens in the magnetotail and is the driver of storms and substorms. Density cavity, also called density depletion layer, is a typical characteristic of magnetic reconnection [*Shay et al.*, 2001]. It is often observed by the spacecraft in the separatrix region of magnetic reconnection [*Mozer et al.*, 2002; *Vaivads et al.*, 2004;

[1]Key Laboratory of Ionospheric Environment, Institute of Geology and Geophysics, Chinese Academy of Sciences, Beijing, China.
[2]Space Research Institute, Austrian Academy of Sciences, Graz, Austria.
[3]Department of Geophysics and Planetary Science, University of Science and Technology of China, Hefei, China.
[4]Swedish Institute of Space Physics, Uppsala, Sweden.
[5]Max Planck Institute for Solar System Research, Katlenburg-Lindau, Germany.
[6]Mullard Space Science Laboratory, Surrey, UK.

Corresponding author: R. Wang, Key Laboratory of Ionospheric Environment, Institute of Geology and Geophysics, Chinese Academy of Sciences, Beijing 100029, China. (Rongsheng.Wang@mail.iggcas.ac.cn)
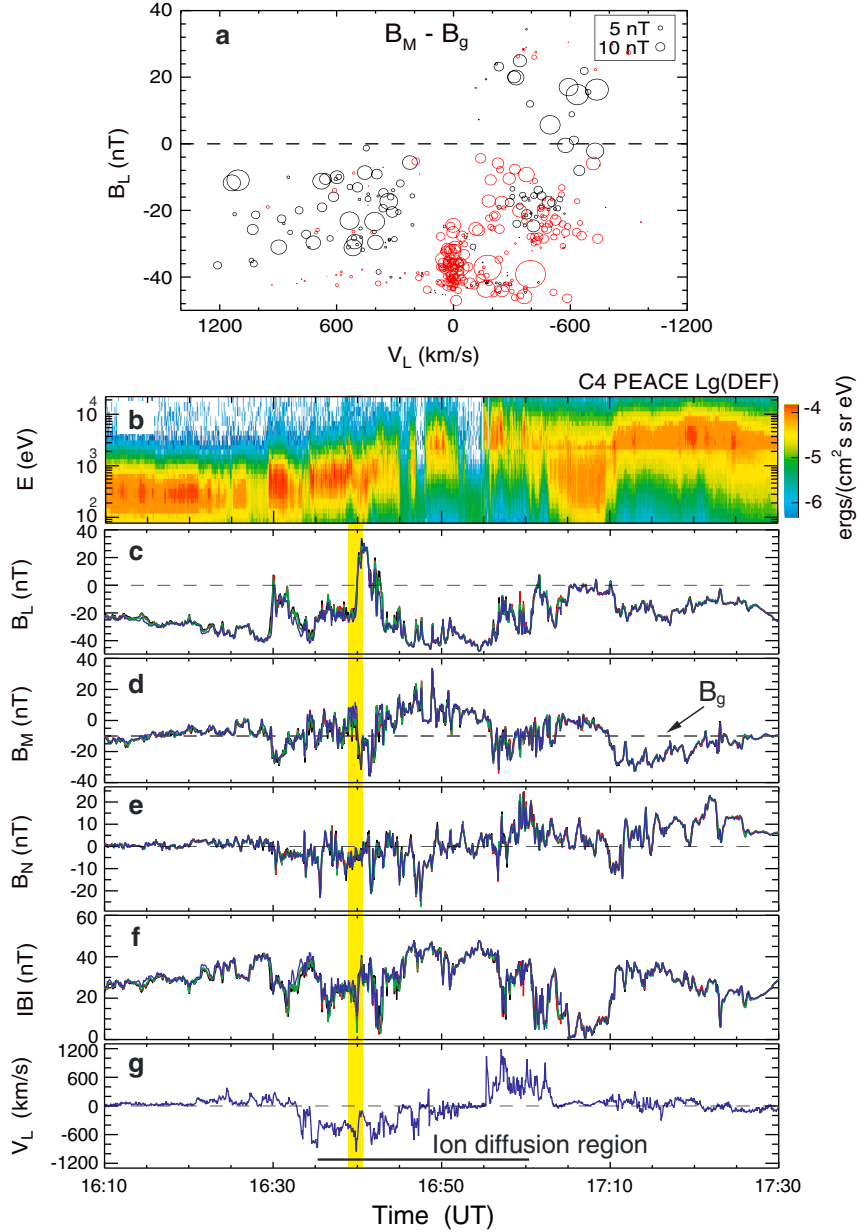
Khotyaintsev et al., 2006; *Retinò et al.*, 2006; *Lu et al.*, 2010; *Zhou et al.*, 2011; *Wang et al.*, 2012] and might play a key role in accelerating electrons [*Drake et al.*, 2005; *Divin et al.*, 2012; *Wang et al.*, 2012]. Within the density cavity, streaming of low energy electrons as a part of Hall current system is detected frequently [*Nagai et al.*, 2001; *Nakamura et al.*, 2008; *Wang et al.*, 2010]. Recently, *Wang et al* [2012] found that the energy of the streaming can be as high as 20 keV. The observations indicate that electrons may have been pre-accelerated in the separatrices. However, the fine structure and how electrons are accelerated in the cavity are still open questions.

[3] In this letter, we present a reconnection event observed by Cluster [*Escoubet et al.*, 1997] in the magnetotail and analyze the density cavity in detail during one simple crossing tailward of the X line. Except for a series of patchy parallel electric field observed in the cavity, the prominent signature of very strong oscillating perpendicular electric field component is measured, which provides a new insight into the acceleration mechanism of electrons in the separatrix.

2. Observation and Analysis

[4] We have used data from various instruments onboard Cluster. The magnetic field data are obtained from the FGM instruments sampled at 0.25/s and at 67/s. The electric field data are taken from the EFW instruments sampled at 450/s. The low-medium (27 eV ~ 22 keV) and high-energy (>41 keV) electron data are taken from the PEACE instruments and the RAPID instruments, respectively. The ion plasma data are obtained from the CIS (CODIF) instruments in 4 s resolution.

[5] Figure 1 shows an overview of the magnetic reconnection event encountered by Cluster on 17 August 2003, at about $[-17, -6, 3]\ R_E$ (Earth radius) in the geocentric solar magnetospheric coordinate system (GSM) with a separation of 200 km (the top panel in Figure 3). To avoid influence of the Hall current system in ion diffusion region, we applied minimum variance analysis (MVA) [*Schwartz*, 1998] to the magnetic field data of the magnetotail current sheet crossing between 1550 and 1620 UT when the current sheet is quiet. Relative to GSM, $L = (0.957,\ 0.237,\ -0.166)$, $M = (-0.271,\ 0.935,\ -0.228)$, and $N = (0.102,\ 0.263,\ 0.959)$, which are used throughout this letter unless otherwise stated. During 1630–1705 UT, the coincident reversals of the high-speed flow from tailward to earthward (Figure 1g) and of the magnetic field component B_N from southward to northward (Figure 1e) are obvious. Simultaneously, there is a background magnetic field in the M direction, a so-called guide field (B_g), of approximately −10 nT. This guide field might originate from the interplanetary magnetic field, as suggested by *Nakamura et al.* [2008]. The scatterplot of

Figure 1. Overview of the magnetic reconnection event. (a) $B_M - B_g$ as a function of B_L and V_L. B_g is the guide field. Sizes of the circles denote magnitude of $B_M - B_g$. The colors black and red correspond to negative and positive values, respectively. The data are obtained from C4 during 16:35–17:00 UT. (b) Electron energy spectrum from HEEA and LEEA at C4. (c–f) Three components and magnitude of magnetic field at the four satellites with a normal color scheme. (g) Proton burst bulk flows in the L component. The vertical yellow bar represents the crossing tailward of X line.

$B_M - B_g$ as a function of V_L and B_L obtained from C4 between 1635 and 1700 UT (horizontal black bar in Figure 1g) is shown in Figure 1a. It is evident that $B_M - B_g$ displays a quadrupolar structure with the upper right quadrant extending down to $B_L \approx -6$nT. The distortion of the quadrupolar structure is caused by the guide field [*Wang et al.*, 2012]. Based on these observations, we conclude that Cluster encountered one reconnection ion diffusion region from the tailward side to the earthward side of the X line. At the tailward side (1635–1645 UT), it crossed the ion diffusion region twice, from south to north and then back to south again. Here we mainly concentrate on the first direct crossing (vertical yellow bar) of which an expanded view is shown in Figure 2.

[6] Figures 2a–2h represent the Cluster data during the simple south-north crossing. The electron density shown in Figure 2a is derived from the spacecraft potential [*Pedersen et al.*, 2008]. In this interval, Cluster crossed the ion diffusion region from $B_L \approx -25$nT to ≈ 40 nT. Simultaneously, $B_M - B_g$ changed signs from positive to negative. It is clear from Figure 1a that the Hall magnetic field $B_M - B_g$ extends to $B_L \approx -40$ nT, much smaller than the starting point of the crossing at $B_L \approx -25$ nT. This means that Cluster only partially crossed the ion diffusion region and did not encounter the southern separatrix. This conclusion can be verified by the current density as well. If Cluster had passed through the southern separatrix, the positive parallel current caused by inflowing electrons should have been observed.
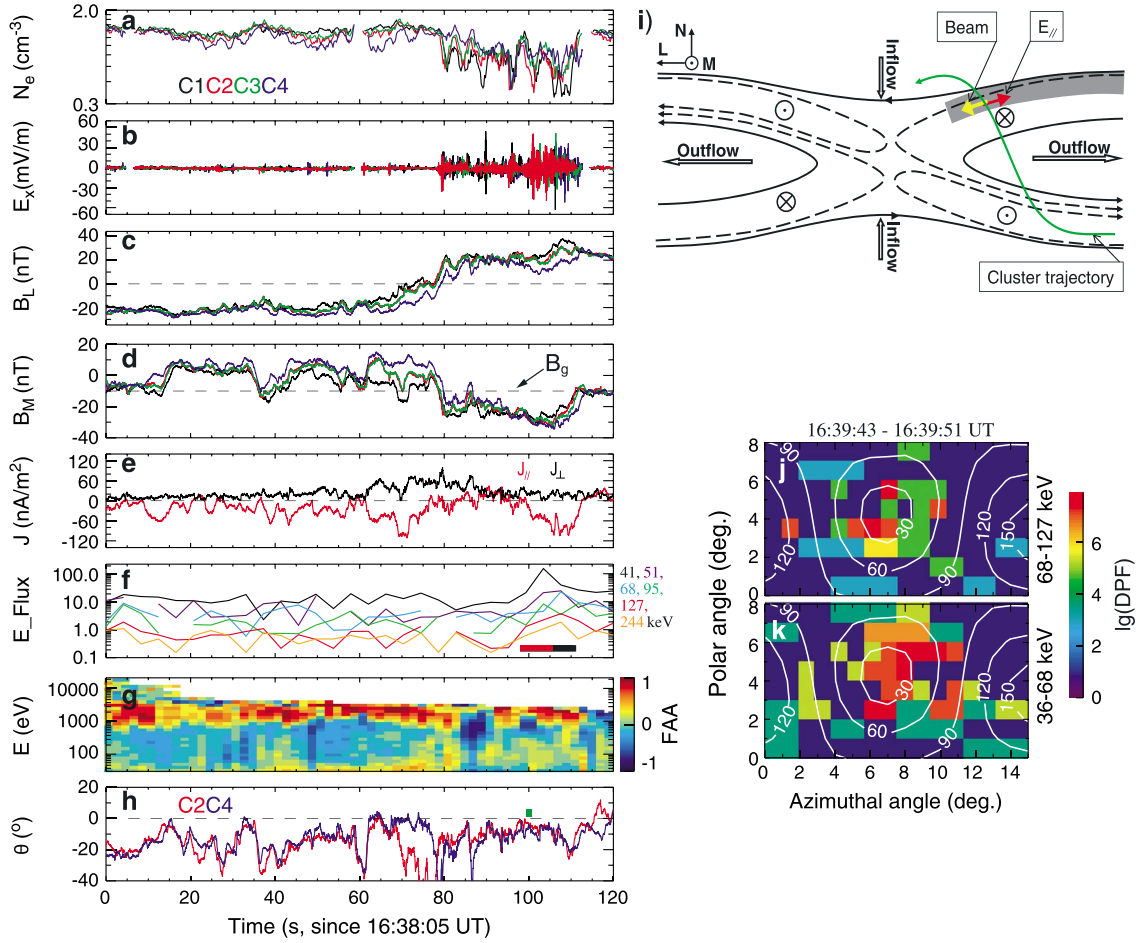
Figure 2. Plasma data during the crossing. (a) Electron density derived from the spacecraft potential. (b) The x components of electric field in the ISR2 coordinates. (c–d) Magnetic field in the L and M components. (e) The parallel (red) and perpendicular components of current density. (f) Fluxes of energetic electrons at C4 in six energy channels. (g) Electron field-aligned anisotropy (FAA) at C4, defined as $(f_p - f_a)/(f_p + f_a)$, where f_p and f_a are phase space densities parallel and antiparallel to magnetic field, respectively. (h) Angles between magnetic field and the spacecraft spin plane. (i) Schematic illustrator for this reconnection event. The green curve denotes the spacecraft trajectory. The shadow area means the density cavity. The red and yellow arrows within it denote the observed unipolar $E_{\parallel}$ and high-energy electron beam, respectively. The dashed lines with arrows are the Hall electron flows. (j–k) 3-D electron differential particle flux (DPF) distribution for two energy levels (36–68 keV and 68–127 keV) at C4. Superimposed white curves are the different pitch angle contours. The horizontal bar with black and red colors in Figure 2f denotes the time with high-energy electron beam observed.

However, the current density was always negative in the Southern Hemisphere (Figure 2e). The Cluster trajectory relative to the ion diffusion region is displayed in Figure 2i.

[7] During this crossing, a thin current layer is observed between $100 \sim 115$ s (Figure 2e). The current is primarily antiparallel to the magnetic field, and its intensity reaches up to -100 nA/m^2, comparable to that observed in the central plasma sheet at about 70 s. This current layer is right observed in the outer boundary of the Hall magnetic field (Figure 2d), i.e., at the northern separatrix as the shaded region in Figure 2i. The current density is estimated by the curlometer technique with the 200 km separation of the Cluster tetrahedron sufficiently smaller than the general thickness of the magnetotail current sheet. The ratio of $\nabla \cdot \mathbf{B}/|\nabla \times \mathbf{B}|$ is below 0.25 while the main two current layers are observed. Thus, the curlometer technique is valid. Figure 2g shows electron field-aligned anisotropy (FAA) taken from the HEEA sensor of PEACE at C4. It is evident that there is a net streaming of electrons parallel to magnetic

field in the current layer. The energy of the streaming electrons is between 1 keV and 3 keV. For electrons with energies larger than 3 keV, there are no available data in parallel and/or antiparallel directions from the PEACE instrument. So the FAA data above 3 keV in Figure 2g are gap. The streaming electrons are consistent with the obtained current density. Thus, we interpret that the current layer in the separatrix is formed by the inflow electrons, as a part of the Hall current system.

[8] During this crossing of the ion diffusion region, electron density decreases when Cluster approaches the northern separatrix (Figure 2a) between 80 and 115 s. Moreover, magnetic field has its maximum value within the density depletion region. An expanded view of the density depletion region is displayed in Figure 3. The observations are in good agreement with the observations of the density cavity in previous literature [*Mozer et al.*, 2002; *Vaivads et al.*, 2004; *Retinò et al.*, 2006; *Khotyaintsev et al.*, 2006; *Lu et al.*, 2010; *Huang et al.*, 2010; *Zhou et al.*, 2011;
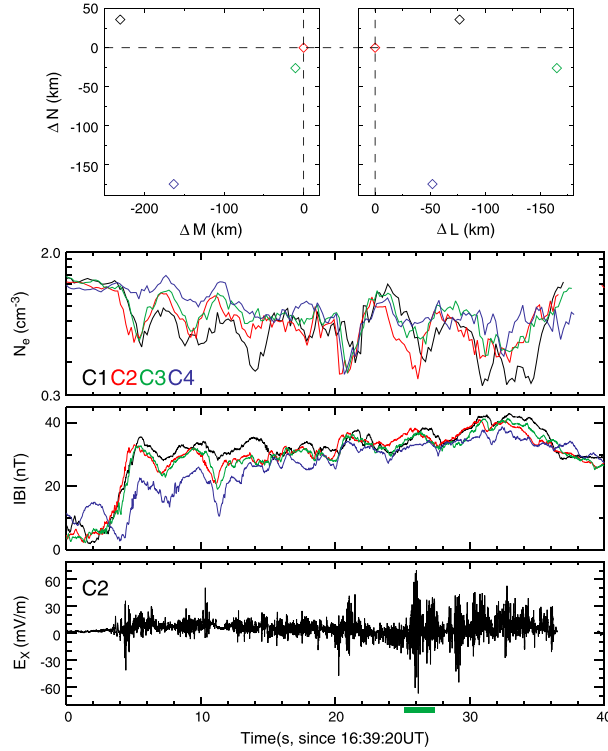
Figure 3. Relative positions of the four satellites at 16:39:40 UT, electron density, magnetic field intensity at the four satellites, and *x* component of electric field from C2 are displayed from top to bottom. The green bar in the bottom corresponds to the time interval shown in Figure 4.

Wang et al., 2012]. In this event, however, the density cavity is distributed over a wide range from $B_L \approx 25$ nT to ≈ 40 nT and not only at the location of the separatrix as expected from the previous literature. Furthermore, six electron density dips with a further density decrease were observed within the cavity (Figures 2a and 3). The average duration of the dips is about 2 s. The largest one is approximate 5 s and observed at the northern separatrix current layer. They are observed as Cluster travels the Hall magnetic field region gradually. The last three dips are respectively observed out of, in the boundary of, and within the northern separatrix current layer (Figures 2a and 2e). In other words, they are located in different spatial location. Moreover, all four satellites observe each one successively. So the last three density dips are separate spatial structures rather other temporal signals. As for the first three dips, they are observed while B_L fluctuates noticeably. It seems that these dips are produced due to one single cavity sweeping the four satellites back and forth. If so, the spacecraft would observe the dips in the order of "first in, first out" or "first in, last out." However, the fact is that the spacecraft enters and exits the dips in disorder. So the dips should be three dimensional and irregular structures. We will call these "sub-cavities." The six sub-cavities are always observed by the four satellites except the third one. Hence, the width of the sub-cavity is comparable to the separation of Cluster at the moment, about 200 km $\sim$ 0.6 c/ω_{pi} (ion inertial length, $N = 0.4$ cm^{-3}). Multiple density sub-cavities adjacent to one single separatrix during reconnection have never been observed before. The physical mechanism will be discussed later.

[9] Electric field fluctuations become substantially strong while the density cavity is observed. Figure 2b shows E_x in the spacecraft spin plane coordinates, called Inverted Spin Reference system (ISR2). E_y shows the similar characteristic (not shown here). The electric field fluctuations are further enhanced and become the largest within the sub-cavities, and the amplitude reaches up to 60 mV/m (Figures 2b and 3). The close correlation between the sub-cavities and the strong electric field fluctuations is very clear in Figures 3. In previous studies, these broadband electrostatic emissions are thought to be formed by electrostatic solitary waves/electron holes [*Matsumoto et al.*, 2003].

[10] Corresponding to the current layer in the northern separatrix, the fluxes of high-energy electrons from 41 to 244 keV are significantly enhanced (Figure 2f). The electron pitch angle distributions in the two energy channels of 68–127 keV and 36–68 keV during this short interval are analyzed in detail also. The electron differential particle fluxes (DPFs) in 0° direction are dramatically larger than other directions between 98 and 112 s (the red and black bars in Figure 2f). That means there is a net high-energy electron inflow in the northern separatrix. The electron pitch angle distribution in a short interval of 8 s (the red bar in Figure 2f) is provided in Figures 2j and 2k showing the 3-D electron intensity distribution. The superimposed white curves are the different pitch angle contours. It is obvious from Figures 2j and 2k that between 36 and 127 keV, there is a net streaming of electrons parallel to the magnetic field. In other words, the high-energy electrons are being injected into the X line. The observations indicate that the electrons have been accelerated effectively whilst they are flowing into the X line along the separatrix.

[11] Recently, *Wang et al.* [2012] have confirmed that the inflow electron in the separatrix could be pre-accelerated up
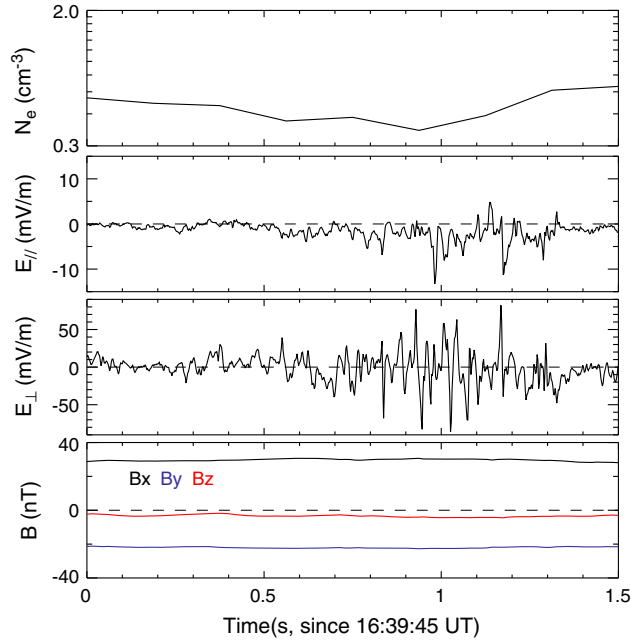
Figure 4. Electron density, electric field in the parallel and perpendicular directions, and three components of magnetic field in the Inverted Spin Reference (ISR2) are shown from top to bottom. The interval denotes the green bar in Figure 2h.

to 20 keV before they enter into the X line. In this current letter, we further demonstrate that the inflow electrons are pre-accelerated to an even higher energy of about 100 keV. How electrons are accelerated in the separatrix is still an issue. Since Cluster only measures two components of the electric field in the spacecraft spin plane, it is almost impossible to get the electric field in parallel and perpendicular directions. However, we still have a chance to get the parallel and perpendicular electric field components ($E_{\parallel}$ and $E_{\perp}$), during periods in which the magnetic field is mainly lying in the spacecraft spin plane. Figure 2h represents the angles between the magnetic field and the spacecraft spin plane. There are several intervals during which the angles are close to zero. Especially, within the current layer in the northern separatrix, there is a short span of 1.5 s, corresponding to the green bar in Figure 2h and in the bottom of Figure 3 also, when the angles are smaller than 7° at C2. Two components of electric field $E_{\parallel}$ and $E_{\perp}$ in the spacecraft spin plane are presented in Figure 4.

[12] Figure 4 shows electron density, $E_{\parallel}$ and $E_{\perp}$ in the spacecraft spin plane, and three components of magnetic field in the ISR2 coordinate system at C2. In this short interval of 1.5 s, C2 is within one of the sub-cavities and the magnetic field there is mainly in the spin plane. So we can calculate the parallel and perpendicular electric field $E_{\parallel}$ and $E_{\perp}$. Within the sub-cavity, a series of patchy parallel electric component are detected. $E_{\parallel}$ is negative, its duration is about tens of milliseconds, and its minimum values is about -10 mV/m. Accompanying with the patchy $E_{\parallel}$, very strong oscillating signatures of $E_{\perp}$ are detected. The amplitude of the oscillating $E_{\perp}$ extends to 80 mV/m. In previous studies, only bipolar $E_{\parallel}$ signatures interpreted as electrostatic solitary waves or electron holes were observed in the separatrix [*Cattell et al.*, 2005; *Matsumoto et al.*, 2003]. In this event, however, no bipolar $E_{\parallel}$ signatures are measured in this short interval. Instead, very strong oscillating perpendicular components and nearly unipolar parallel component are measured. On the other hand, in the Southern Hemisphere
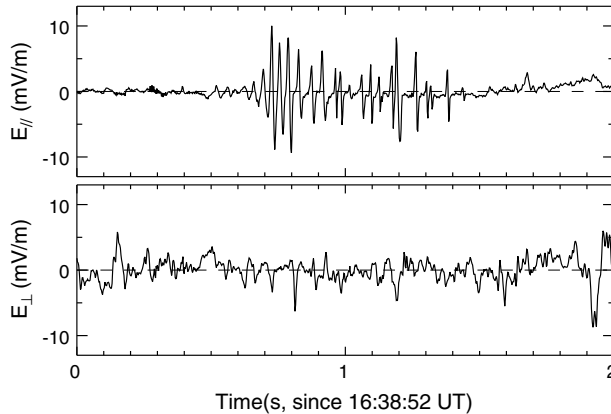

Figure 5. Electric field in parallel and perpendicular directions during 2 s.

away from the separatrix, we do find bipolar $E_{\parallel}$ signatures, as shown in Figure 5. The bipolar $E_{\parallel}$ signatures are a common feature in the Southern Hemisphere. They can be detected almost everywhere except very close to the center of the plasma sheet ($B_x > -10\,\text{nT}$). The typical value of the bipolar $E_{\parallel}$ signatures is about 3 mV/m and the biggest is 8 mV/m shown in Figure 5. For other intervals with angles close to zero (mainly in the Southern Hemisphere) in Figure 2h, no reliable unipolar $E_{\parallel}$ is observed.

3. Discussion

[13] Electron density cavities are typical characteristics during magnetic reconnection. Generally, only one single density cavity lies along the separatrix. In our event, however, multiple sub-cavities within the density decrease region are observed adjacent to the separatrix. At the magnetopause, two density dips are observed in the side of the magnetosphere while the spacecraft crossed the magnetopause [*Lindstedt et al.*, 2009], where they attributed the two density dips to simultaneous occurrence of two reconnection X lines. Recent simulation studies proposed that the density fluctuations grow within the cavity due to the electron Kelvin-Helmholtz (KH) instability [*Divin et al.*, 2012]. In three-dimensional simulations, the lower density depletion layers called low density ribs develop within the normal cavity [*Markidis et al.*, 2012]. In a certain degree, the observed sub-cavities resemble the simulation results. The electron KH instability will result in the density perturbation with a scale of $0.2c/\omega_{pi}$, which is basically consistent with our observations also. So the electron KH instability is one plausible candidate for the formation of the observed sub-cavities. Within the density sub-cavities, electric field fluctuations become very strong. Using the electric field data in a short interval (within one of the sub-cavities) when the data can be divided into the parallel and perpendicular components, we find that the strong electric field fluctuations are mainly produced by the oscillating perpendicular components. Relative to the oscillating perpendicular component, the parallel electric field component is weak and nearly unipolar and directs away the X line. The oscillating perpendicular electric field may be related to the lower hybrid drift waves [*Krall and Liewer*, 1971]. Such waves are commonly detected in the region with a gradient of plasma density and magnetic field and account for the strong perpendicular electric field [*Norgren et al.*, 2012].

[14] In the northern separatrix, a high-energy electron beam up to 100 keV is observed. This beam is injected into the X line along the magnetic field. The observation indicates that electrons flowing into the X line have been pre-accelerated effectively along the separatrix. In the same region, a unipolar parallel electric field directed away from the X line is observed, from which we deduce that the observed inflow electrons are accelerated by this parallel electric field. A schematic is shown in Figure 2i. The four satellites crossed the separatrix successively. However, only C4, which crosses the separatrix at last, observes the high-energy electron inflow. The reason is still unclear. One possible reason is that the beam is very narrow and only C4 detects it. Another reason is that the high-energy electron beam is intermissive due to the electron Kelvin-Helmholtz instability as in simulations [*Divin et al.*, 2012] and only C4 encounters it. The patchy parallel electric field is also observed in the boundary of the reconnection outflow far

away from X line at the magnetopause [*Mozer et al.*, 2010]. So it might be a common feature in the separatrix.

[15] The energy of the observed electron beam is so high that Buneman instability will be excited. Then, electron holes will be created there according to the theory [e.g., *Divin et al.*, 2012]. However, within the sub-cavity, no bipolar parallel electric field is observed in our event. The reason is still unclear. In the simulations, *Markidis et al.* [2012] found that the electron holes just appear in the higher-density region of the cavities (between the low density ribs). In our event, we get $E_{\parallel}$ and $E_{\perp}$ only within one of the sub-cavities, which might be the reason for the absence of electron holes in our event. Another possible reason is that the electron holes in the Northern Hemisphere have less time scale than the spacecraft time resolution and cannot be resolved. In contrast, electron holes are measured almost everywhere in the Southern Hemisphere except near the central plasma sheet.

4. Conclusions

[16] We have investigated one direct south-north crossing of an ion diffusion region. Multiple electron density sub-cavities are first observed adjacent to the north separatrix where a current layer is observed also. The remarkable characteristic during this event is the correlation between the electron sub-cavities and the strong electric field fluctuations. From the strong electric fluctuations in one of the sub-cavities within the northern separatrix current layer, we find that the fluctuations primarily come from the oscillating perpendicular components, and the parallel electric field component is nearly unipolar and directs away the X line. At the same time, in addition to the low-medium energy electron streaming flowing into the X line along magnetic field, a high-energy electron beam up to 100 keV is injected into the X line also. It seems that the observed high-energy electron beam is accelerated by the unipolar parallel electric field.

[18] The Editor thanks two anonymous reviewers for their assistance in evaluating this paper.

References

Cattell, C., et al. (2005), Cluster observations of electron holes in association with magnetotail reconnection and comparison to simulations, *J. Geophys. Res.*, *110*, A01211, doi:10.1029/2004JA010519.

Divin, A., G. Lapenta, S. Markidis, D. L. Newman, and M. V. Goldman (2012), Numerical simulations of separatrix instabilities in collisionless magnetic reconnection, *Phys. Plasmas*, *19*, 042110, doi:10.1063/1.3698621.

Drake, J. F., M. A. Shay, and W. Thongthai (2005), Production of energetic electrons during magnetic reconnection, *Phys. Rev. Lett.*, *94*, 095001, doi:10.1103/PhysRevLett.94.095001.

Escoubet, C. P., R. Schmidt, and M. L. Goldstein (1997), Cluster—Science and mission overview, *Space Sci. Rev.*, *79*, 11–32.

Huang, C., Q. M. Lu, and S. Wang (2010), The mechanisms of electron acceleration in antiparallel and guide field magnetic reconnection, *Phys. Plasmas*, *17*, 072306, doi:10.1063/1.3457930.

Khotyaintsev, Y. V., A. Vaivads, A. Retino, and M. Andre (2006), Formation of inner structure of a reconnection separatrix region, *Phys. Rev. Lett.*, *97*(20), doi:10.1103/PhysRevLett.97.205003.

Krall, N. A., and P. C. Liewer (1971), Low-frequency instabilities in magnetic pulses, *Phys. Rev. A*, *4*(5), 2094–2103.

Lindstedt, T., Y. V. Khotyaintsev, A. Vaivads, M. Andre, R. C. Fear, B. Lavraud, S. Haaland, and C. J. Owen (2009), Separatrix regions of magnetic reconnection at the magnetopause, *Ann. Geophys.*, *27*(10), 4039–4056.

Lu, Q. M., C. Huang, J. L. Xie, R. S. Wang, M. Y. Wu, A. Vaivads, and S. Wang (2010), Features of separatrix regions in magnetic reconnection: Comparison of 2-D particle-in-cell simulations and Cluster observations, *J. Geophys. Res.*, *115*, A11208, doi:10.1029/2010JA015713.

Markidis, S., G. Lapenta, A. Divin, M. Goldman, D. Newman, and L. Andersson (2012), Three-dimensional density cavities in guide field collisionless magnetic reconnection, *Phys. Plasmas*, *19*, doi.org/10.1063/1.3697976.

Matsumoto, H., X. H. Deng, H. Kojima, and R. R. Anderson (2003), Observation of electrostatic solitary waves associated with reconnection on the dayside magnetopause boundary, *Geophys. Res. Lett.*, *30*(6), 1326, doi:10.1029/2002GL016319.

Mozer, F. S., S. D. Bale, and T. D. Phan (2002), Evidence of diffusion regions at a subsolar magnetopause crossing, *Phys. Rev. Lett.*, *89*, doi:10.1103/PhysRevLett.89.015002.

Mozer, F. S., and P. L. Pritchett (2010), Spatial, temporal, and amplitude characteristics of parallel electric fields associated with subsolar magnetic field reconnection, *J. Geophys. Res.*, *115*, A04220, doi:10.1029/2009JA014718.

Nagai, T., I. Shinohara, M. Fujimoto, M. Hoshino, Y. Saito, S. Machida, and T. Mukai (2001), Geotail observations of the Hall current system: Evidence of magnetic reconnection in the magnetotail, *J. Geophys. Res.*, *106*(A11), 25929–25949.

Nakamura, R., et al. (2008), Cluster observations of an ion-scale current sheet in the magnetotail under the presence of a guide field, *J. Geophys. Res.*, *113*, A07S16, doi:10.1029/2007JA012760.

Norgren, C., A. Vaivads, Y. V. Khotyaintsev, and M. Andre (2012), Lower hybrid drift waves: Space observations, *Phys. Rev. Lett.*, *109*, doi:10.1103/PhysRevLett.109.055001.

Pedersen, A., et al. (2008), Electron density estimations derived from spacecraft potential measurements on Cluster in tenuous plasma regions, *J. Geophys. Res.*, *113*, A07S33, doi:10.1029/2007JA012636.

Retinò, A., et al. (2006), Structure of the separatrix region close to a magnetic reconnection X-line: Cluster observations, *Geophys. Res. Lett.*, *33*, L06101, doi:10.1029/2005GL024650.

Schwartz, S. J. (1998), Shock and discontinuity normals, Mach numbers, and related parameters, in *Analysis Methods for Multi Spacecraft Data*, edited by G. Paschmann and P. W. Daly, 256 p., Eur. Space Agency, Bern Switzerland.

Shay, M. A., J. F. Drake, B. N. Rogers, and R. E. Denton (2001), Alfvenic collisionless magnetic reconnection and the Hall term, *J. Geophys. Res.*, *106*(A3), 3759–3772.

Vaivads, A., Y. Khotyaintsev, M. Andre, A. Retino, S. C. Buchert, B. N. Rogers, P. Decreau, G. Paschmann, and T. D. Phan (2004), Structure of the magnetic reconnection diffusion region from four-spacecraft observations, *Phys. Rev. Lett.*, *93*, doi:10.1103/PhysRevLett.93.105001.

Wang, R. S., Q. M. Lu, C. Huang, and S. Wang (2010), Multispacecraft observation of electron pitch angle distributions in magnetotail reconnection, *J. Geophys. Res.*, *115*, A01209, doi:10.1029/2009JA014553.

Wang, R. S., et al. (2012), Asymmetry in the current sheet and secondary magnetic flux ropes during guide field magnetic reconnection, *J. Geophys. Res.*, *117*, A07223, doi:10.1029/2011JA017384.

Zhou, M., Y. Pang, X. H. Deng, Z. G. Yuan, and S. Y. Huang (2011), Density cavity in magnetic reconnection diffusion region in the presence of guide field, *J. Geophys. Res.*, *116*, A06222, doi:10.1029/2010JA016324.